recommending any particular number of mixes. We designed the workcell's 6-axis robot to perform the mixing by maintaining the specimens over a fixed location, so that a stainless steel pan could be positioned to catch drips from any leaking specimens. This design, coupled with the design of the pneumatic tool and its pin cylinders limited the range of rotation of the tubes to 126° in either direction. The resulting mixing pattern consisted of a rotation of approximately 126° to the left from an upright starting position, return to upright, then 126° to the right, and return to upright. A single 126° tilt and return to upright constitutes 1 mix cycle in this discussion.

We evaluated 0, 2, 4, up to 12 mix cycles each with 5 different replicate expired blood bank plasma specimens of 4.5 mL using our standard false bottom tube. The tubes were thawed on the workcell deck, but without the air blowing, to avoid any vibration or shaking of the tubes. After the tubes had thawed, we carefully sampled 200 μL from the uppermost layer of each tube. The 1st set of replicates was sampled without robotic mixing, the 2nd set was sampled after 2 mix cycles, the 3rd set after 4 mix cycles, and so on. The aliquots were analyzed for albumin, sodium, potassium, and chloride on a Modular P analyzer (Roche Diagnostics) and compared to 5 replicates of unfrozen plasma that served as baseline or expected values. The results are shown in Table 1. After only 2 mix cycles (2 elevations to 126° followed by return to upright), the levels of all 4 analytes were indistinguishable from the baseline levels. This result was surprisingly fewer than we had expected based on experience. However, because human mixing motions may not duplicate the uniform speed and angles of our programmed robot (approximately 2 seconds to tilt 126° and return to upright), we are not recommending that laboratorians reduce their specimen mixes.

Knowing that an air bubble was required to achieve specimen mixing, we evaluated overfilling tubes with plasma in an attempt to determine the minimum size of air bubble necessary for adequate mixing. The volume of water expands approximately 9% when it is frozen *(4)*. Furthermore, if a tube is filled too full and leaks due to this expansion, specimen solutes (minerals, proteins, etc.) preferentially squeeze through the cap threads, as has been reported for frozen, overfilled standard solutions *(5)* and for frozen, overfilled serum and urine specimens *(2)*, and leaked specimens will be unacceptable for testing because the concentrations of analytes will have changed. We also learned that the minimum size of air bubble to facilitate mixing was 1.0 mL, which was sufficiently below the top of the tube to prevent leakage during freezing.

In summary, we designed, validated, and installed an automated thawing and mixing workcell, which is connected to our automated transport system and has a throughput to thaw and mix >1000 specimens per hour. The 6-axis robot appears able to effectively mix specimens with fewer mixes than routinely taught to laboratorians. Overfilled specimens that leak when frozen are unacceptable for laboratory analysis.

Grant/funding support: This work was supported by ARUP Laboratories.
Financial disclosures: None declared.

References

1. Buse FW, Karassik IJ, Krutzsch WC, Worster AR, Dayton BB, Jorgensen R. Pumps and compressors. In: Baumeister T, Avallone EA, Baumeister T III, eds. Marks' Standard Handbook for Mechanical Engineers, 8th ed. New York: McGraw Hill, 1978(Chapt 14):14-30–14-44.
2. Omang SH, Vellar OD. Concentration gradients in biological samples during storage, freezing and thawing. Z Anal Chem 1974;269:177–81.
3. Hirano T, Yoneyama T, Matsuzaki H, Sekine T. Simple method for preparing a concentration gradient of serum components by freezing and thawing. Clin Chem 1991;37:1225–9.
4. Ophardt CE. Elmhurst College, Virtual ChemBook. http://www.elmhurst.edu/~chm/vchembook/122Adensityice.html (accessed June 2007).
5. McGlory DH. Often-overlooked effect of freezing standard solutions [Letter]. Clin Chem 1971;17:1074.

Previously published online at DOI: 10.1373/clinchem.2007.094185

Detection of Factor VIII Gene Mutations by High-Resolution Melting Analysis, *Andrew D. Laurie,* Mark P. Smith, and Peter M. George* (Department of Molecular Pathology, Canterbury Health Laboratories, Christchurch, New Zealand; * address correspondence to this author at: P.O. Box 151, Christchurch, New Zealand; fax 64-3-3640545, e-mail andrew.laurie@cdhb.govt.nz)

Background: **Single base-pair substitution mutations in the gene for coagulation factor VIII, procoagulant component (hemophilia A) (*F8*) account for approximately 50% of severe cases of hemophilia A (HA), and almost all moderate or mild cases. Because *F8* is a large gene, mutation screening using denaturing HPLC or DNA sequencing is time-consuming and expensive.**

Methods: **We evaluated high-resolution melting analysis as an option for screening for *F8* gene mutations. The melting curves of amplicons heterozygous for known *F8* gene mutations were compared with melting curves of the corresponding normal amplicons to assess whether melting analysis could detect these variants. We examined 2 platforms, the Roche LightCycler 480 (LC480) and the Idaho Technology LightScanner.**

Results: **On both instruments, 18 (90%) of the 20 *F8* gene variants we examined were resolved by melting analysis. For the other 2 mutations, the melting curves of the heterozygous amplicons were similar to the corresponding normal amplicons, suggesting these variants may not be detected by this approach in a mutation-scanning screen.**

Conclusion: **High-resolution melting analysis is an appealing technology for *F8* gene screening. It is rapid and quickly identifies mutations in the majority of HA patients; samples in which no mutation is detected require further testing by DNA sequencing. The LC480 and LightScanner platforms performed similarly.**

Hemophilia A (HA) is a coagulation disorder caused by a lack of normal coagulation factor VIII (FVIII) activity *(1)*. This disease is caused by mutations in the coagulation factor VIII, procoagulant component (hemophilia A) (*F8*) gene, which encodes FVIII and is located at Xq28. *F8* is a large gene, comprising 26 exons across 186 kb, and produces a 9-kb mRNA transcript. All exons are small (69–262 bp) except exon 14, which is 3.1 kb.

Approximately 45% of severe HA cases are the result of a large inversion that disrupts the *F8* gene in intron 22, and a further 1%–5% are caused by an inversion affecting intron 1. In the remaining severe cases, and in cases of mild or moderate HA, a single-base substitution, small insertion, or deletion is usually the causative mutation. Such mutations create either missense, nonsense, or frameshift mutations, or affect consensus splice sites [reviewed in *(2)*]. Many such variants have been reported in HA patients, and more than 900 different mutations have been described *(3)*.

Many hematology services now offer genetic screening to identify the *F8* gene mutation in their HA patients. This information allows identification of carrier females, prenatal testing for affected pregnancies, preimplantation genetic diagnosis, and in some cases prediction of the likelihood of FVIII inhibitor production in HA patients receiving prophylactic FVIII treatment *(2)*.

Genetic screening of HA patients who do not have either the intron 1 or intron 22 inversions is problematic because of the size of the *F8* gene and the variety of mutations that can occur. Before capillary-based DNA sequencing platforms were widely available it was not practical to sequence all 26 exons, so mutation-scanning strategies such as single-strand conformational polymorphism analysis were used *(4)*. A more sensitive technique, denaturing HPLC (dHPLC), has also been used successfully for *F8* mutation scanning *(5)*. In our laboratory we have used dHPLC combined with DNA sequencing to identify 20 different *F8* gene mutations in 28 HA patients we have analyzed *(6)*. Although we have found dHPLC to be a sensitive scanning method, it is a low-throughput technology and has many ongoing costs. Likewise, DNA sequencing of the *F8* gene is time-consuming and expensive.

High-resolution melting analysis represents the next generation of mutation scanning technology and offers considerable time and cost savings over both dHPLC and sequencing. This closed-tube assay is performed on amplicons post-PCR. In the presence of a saturating double-stranded DNA-binding dye, amplicons are slowly heated until fully denatured while the fluorescence is monitored *(7)*. Amplicons heterozygous for a sequence variant yield altered melting curves compared with normal control samples. High-resolution melting analysis has recently been tested in a variety of clinical mutation-scanning applications and shown to be a sensitive and cost-effective technique *(8–14)*.

In this study we assessed whether 20 different *F8* gene mutations, located across 13 exons, could be detected by high-resolution melting analysis. These are mutations we have previously identified by dHPLC and DNA sequencing during our *F8* gene-screening program *(6)*. For each mutation we assessed whether the melting curve of the heterozygous amplicon differed from that of the corresponding normal amplicon to evaluate whether a melting analysis screen of the F8 gene would detect the variant. We tested 2 different platforms—the Roche LightCycler 480 (LC480) and the Idaho Technology LightScanner.

Genomic DNA from 20 male HA patients, each with a different *F8* gene mutation, was mixed with an equal amount of DNA from a healthy male control. Because males are hemizygous for the *F8* gene, this mixing is necessary to ensure the amplified exon is heterozygous for the *F8* mutation, which is a requirement for detection by melting analysis. Each mixed sample, and a mixed normal control, was amplified using primers targeting only the *F8* exon where the mutation is located. We used primer sets previously optimized for dHPLC by Oldenburg et al. *(5)*, because the requirements of amplicons for melting analysis are likely to be similar to those for dHPLC. Samples were amplified in duplicate 15-μL PCRs using the LightCycler 480 Genotyping Master PCR mixture (Roche), in the presence of 1× LCGreen PLUS (Idaho Technology), 0.5 μmol/L forward and reverse primers, and 50 ng DNA template. The thermal cycling protocol was as follows: polymerase activation (95 °C for 10 min); touchdown cycling step [5 cycles of: denaturation at 95 °C for 20 s, annealing at 61 °C for 20 s (decreased by 1 °C per cycle), extension at 72 °C for 20 s]; amplification (40 cycles of: denaturation at 95 °C for 20 s, annealing at 56 °C for 20 s, extension at 72 °C for 20 s); and a final extension (72 °C for 5 min). The touchdown cycling step was included to improve specificity of the PCR because LCGreen PLUS is known to increase the melting temperature of primers by 2–4 °C *(15)*. For samples analyzed on the LC480, the melting step was appended to the amplification step; samples melted on the LightScanner were amplified on the LC480 as above, then transferred to the LightScanner for the melting analysis.

To analyze melting data on both the LC480 and the LightScanner software, melting curves were normalized by defining regions in the pre- and postdenaturation parts of the curve, and the value was set for the melting temperature shift adjustment. Output plots are in the form of normalized temperature-shifted melting curves that show the decrease in fluorescence (Fl) against increasing temperature, and difference curves that show the difference in fluorescence (ΔFl) between the melting curves of the mutation sample and the normal control, against temperature. The difference curves provided the best resolution to differentiate mutation and normal samples, with the amplitude of the peak (ΔFl_{max}) recorded as a measure of the resolution. On the basis of the observed

Table 1. Summary of high-resolution melting analysis of 20 *F8* gene variants.

Nucleotide change[a]	Amino acid change[b]	Exon	Amplicon size (bp)	Detected	ΔFl_{max} (LightScanner)[c]	ΔFl_{max} (LC480)[c]
c.1172G>A	R372H	8	338	Yes	0.08	7
c.1409_1418 delCTTTA		9	284	Yes	0.14	12
c.1649C>A	R531H	11	294	Yes	0.17	15
c.1834G>T	R593C	12	230	Yes	0.10	11
c.3864_3870insA		14v[d]	429	Yes	0.08	10
c.4757G>A	W1567X	14vii[d]	436	Yes	0.05	6
c.5380T>C	F1775L	16	330	No	0.03	2
c.5399G>A	R1781H	16	330	Yes	0.06	−5
c.5573C>T	S1839F	16	330	Yes	0.16	17
c.5602T>C	S1849P	17	349	Yes	0.10	12
c.6193T>C	W2046R	21	168	Yes	0.12	12
c.6317A>C	Q2087P	22	206	Yes	0.20	18
c.6449A>T	D2131V	23	250	Yes	−0.05–0.02	5
c.6532C>T	R2159C	23	250	Yes	0.18	16
c.6533G>A	R2159H	23	250	Yes	0.18	16
c.6547A>G	M2164V	23	250	Yes	0.13	11
c.6682C>T	R2209X	24	249	Yes	0.25	22
c.6723 + 1G>C		24[e]	249	Yes	0.17	18
c.6744G>T	W2229C	25	323	Yes	−0.06–0.07	8
c.6901–2A>G		26[e]	217	No	0.04	2

[a] Mutation nomenclature is in accordance with the Human Genome Variation Society guidelines (numbering begins at the "A" nucleotide of the initiating "ATG" codon).

[b] Amino acid numbering uses the classical FVIII system, which starts at the first residue of the mature peptide.

[c] ΔFl_{max} values represent the maximum peak amplitude of the mutation sample difference curve compared to the baseline normal control.

[d] Exon 14 is amplified as 8 overlapping amplicons 14i–14viii.

[e] The splicing variants c.6723 + 1G>C (intron 24) and c.6901-2A>G (intron 25) were detected in the exon 24 and 26 amplicons, respectively, which include flanking intronic regions.

variation in 4 normal controls (see Figs. 1–3 in the Data Supplement that accompanies the online version of this Technical Brief at http://www.clinchem.org/content/vol53/issue12), we considered that a ΔFl_{max} value of at least 5 on the LC480, which is equivalent to 0.05 on the LightScanner, was sufficient resolution to distinguish the mutant sample from the normal control, although the shape of the curve is also an important consideration and may indicate the presence of a variant even if $\Delta Fl_{max} \leq 5/0.05$.

Analysis of the data indicated that 18 of 20 *F8* gene mutations included in this study were detected by melting analysis on both LC480 and LightScanner platforms, with ΔFl_{max} values of at least 5/0.05 (Table 1). The variants F1775L (c.5380T>C, exon 16) and c.6901–2A>G [intron 25 (exon 26 amplicon)] had ΔFl_{max} of $<5/0.05$, indicating a lower confidence in the ability of the melting analysis to resolve the mutant sample from the normal controls (see Figs. 1 and 3 in the online Data Supplement). Even when PCR products from the mutant samples were mixed with products from normal DNA post-PCR, the resolution of these samples was still poor (see Figs. 4 and 5 in the online Data Supplement).

Data for the melting analysis of *F8* exon 23 variants on the LightScanner is shown in Fig. 1. These curves are representative of the other samples in the study listed in Table 1 and show the difference curve for each variant (in duplicate) derived using the normal sample melting curve as a reference, which appears on the difference plot as the baseline. Each exon 23 variant has a distinct curve profile, indicating this technique can distinguish different variants from each other, as well as from the normal sample. Melting curves for these exon 23 variants on the LC480 are shown in Fig. 2 of the online Data Supplement, along with 4 controls to indicate the variability in normal samples.

The LC480 and LightScanner platforms performed similarly overall, although each has strengths and weaknesses. The LC480 is a thermal cycler, so samples for melting analysis can be amplified on this machine, with the melting step appended to the PCR protocol. The amplification of samples can be monitored in real time, because LCGreen PLUS fluorescence is proportional to the amount of double-stranded DNA in the PCR, and any samples in which amplification failed can be removed from the melting analysis. The LightScanner performs only the melting step, but in our hands gave greater consistency between replicate samples. Both machines use a 96-well plate format (with the option for a 384-well format), enabling rapid throughput of samples.

In summary, high-resolution melting analysis is a powerful and cost-effective option for mutation scanning of the *F8* gene. The sensitivity of this technique is comparable to dHPLC, and it offers advantages in the speed and cost of

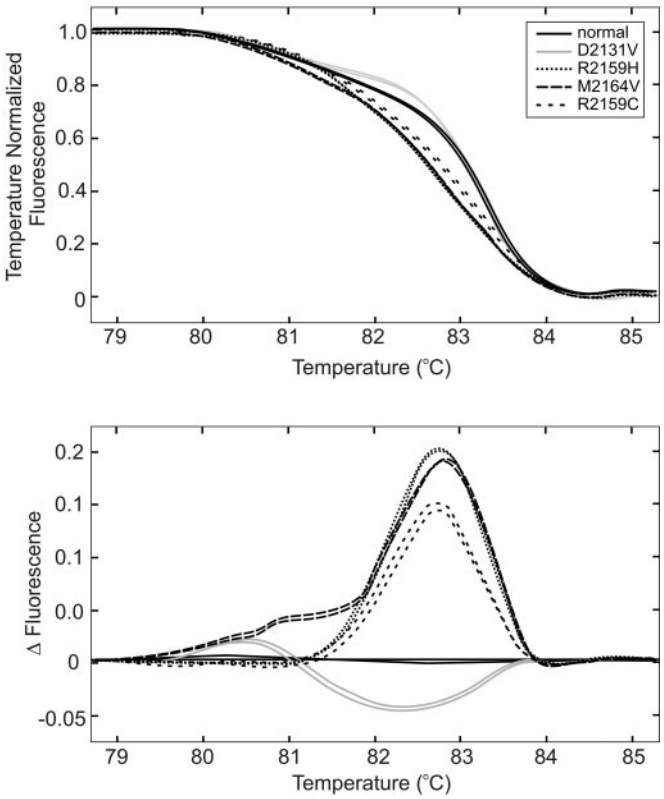

Fig. 1. High-resolution melting curves for the *F8* exon 23 amplicon, showing variants D2131V, R2159C, R2159H, and M2164V, obtained using the LightScanner.

The *upper chart* shows the normalized temperature-shifted melting curves [using the default melting-temperature shift adjustment (0.05)], and the *lower chart* shows the difference curves, derived using the normal sample as the baseline. Data for duplicate samples for each variant is shown. For data from the LC480, see Fig. 2 in the online Data Supplement.

analysis. To support the *F8* mutation-scanning screen in the clinical setting, DNA sequencing of amplicons in which a putative mutation (or polymorphism) was detected can be used to confirm and identify the variant and to rescreen any samples in which no mutations were detected across all *F8* exons. In this context, scanning by high-resolution melting analysis is an ideal technology because it is rapid, economical, and capable of detecting most mutations (90% in this study). Mutations not detected by the melting analysis screen would be identified by subsequent sequencing of all F8 exons for that sample.

Grant/funding support: We acknowledge Roche Diagnostics (New Zealand) for the use of the Roche LC480, and John Morris Scientific for the use of the Idaho Technology LightScanner.
Financial disclosures: None declared.
Acknowledgments: We are grateful to Scott Mead and Campbell Sheen for helpful comments.

References

1. Online Mendelian Inheritance in Man, OMIM (TM). Johns Hopkins University, Baltimore, MD. MIM Number: {306700}: {5/1/2007} http://www.ncbi.nlm.nih.gov/omim/ (accessed June 2007).
2. Graw J, Brackmann H-H, Oldenburg J, Schneppenheim R, Spannag M, Schwaab R. Haemophilia A: from mutation analysis to new therapies. Nat Rev Genet 2005;6:488–501.
3. Kemball-Cook G, Tuddenham EG, Wacey AI. The factor VIII structure and mutation resource site: HAMSTeRS version 4. Nucleic Acids Res 1998;26:216–9.
4. Economou EP, Kazazian HH, Antonarakis SE. Detection of mutations in the factor VIII gene using single-stranded conformational polymorphism (SSCP). Genomics 1992;13:909–11.
5. Oldenburg J, Ivaskevicius V, Rost S, Fregin A, White K, Holinski-Feder E, et al. Evaluation of DHPLC in the analysis of hemophilia A. J Biochem Biophys Methods 2001;47:39–51.
6. Laurie AD, Sheen CR, Hanrahan V, Smith MP, George PM. The molecular aetiology of haemophilia A in a New Zealand patient group. Haemophilia 2007;13:420–7.
7. Wittwer CT, Reed GH, Gundry CN, Vandersteen JG, Pryor RJ. High-resolution genotyping by amplicon melting analysis using LCGreen. Clin Chem 2003;49:853–60.
8. Chou L-S, Lyon E, Wittwer CT. A comparison of high-resolution melting analysis with denaturing high-performance liquid chromatography for mutation scanning: cystic fibrosis transmembrane conductance regulator gene as a model. Am J Clin Pathol 2005;124:330–8.
9. Dobrowolski SF, Ellingson C, Coyne T, Grey J, Martin R, Naylor EW, et al. Mutations in the phenylalanine hydroxylase gene identified in 95 patients with phenylketonuria using novel systems of mutation scanning and specific genotyping based upon thermal melt profiles. Mol Genet Metab 2007;91:218–27.
10. Kennerson ML, Warburton T, Nelis E, Brewer M, Polly P, De Jonghe P, et al. Mutation scanning the GJB1 gene with high-resolution melting analysis: implications for mutation scanning of genes for Charcot-Marie-Tooth disease. Clin Chem 2007;53:349–52.
11. Krypuy M, Newnham GM, Thomas DM, Conron M, Dobrovic A. High resolution melting analysis for the rapid and sensitive detection of mutations in clinical samples: KRAS codon 12 and 13 mutations in non-small cell lung cancer. BMC Cancer 2006;21:6:295.
12. Lonie L, Porter DE, Fraser M, Cole T, Wise C, Yates L, et al. Determination of the mutation spectrum of the EXT1/EXT2 genes in British Caucasian patients with multiple osteochondromas, and exclusion of six candidate genes in EXT negative cases. Hum Mutat 2006;27:1160.
13. Margraf RL, Mao R, Highsmith WE, Holtegaard LM, Wittwer CT. Mutation scanning of the RET protooncogene using high-resolution melting analysis. Clin Chem 2006;52:138–41.
14. Willmore-Payne C, Holden JA, Chadwick BE, Layfield LJ. Detection of c-kit exons 11- and 17-activating mutations in testicular seminomas by high-resolution melting amplicon analysis. Mod Pathol 2006;19:1164–9.
15. LightScanner Instrument Demonstration Guidelines. Idaho Technology Inc., Salt Lake City, Utah.

Previously published online at DOI: 10.1373/clinchem.2007.093781